5782 J. Med. Chem. 2010, 53, 5782–5791
DOI: 10.1021/jm1002974

Journal of Medicinal Chemistry Article

Design of Potent Inhibitors of Human RAD51 Recombinase Based on BRC Motifs of BRCA2 Protein: Modeling and Experimental Validation of a Chimera Peptide

Julian Nomme,[†] Axelle Renodon-Cornière,[†] Yuya Asanomi,[‡] Kazuyasu Sakaguchi,[‡] Alicja Z. Stasiak,[§] Andrzej Stasiak,*[,§] Bengt Norden,[∥] Vinh Tran,[†] and Masayuki Takahashi*[,†]

[†]*UMR 6204 U-3B, Centre National de la Recherche Scientifique & Université de Nantes, F-44322 Nantes cedex 3, France,* [‡]*Department of Chemistry, Faculty of Science, Hokkaido University, 060-0810 Sapporo, Japan,* [§]*Centre Intégratif de Génomique, Faculté de Biologie et de Médecine, Université de Lausanne, CH-1015 Lausanne-Dorigny, Switzerland, and* [∥]*Department of Chemistry and Bioscience, Chalmers University of Technology, SE-412 96 Gothenburg, Sweden*

Received March 6, 2010

We have previously shown that a 28-amino acid peptide derived from the BRC4 motif of BRCA2 tumor suppressor inhibits selectively human RAD51 recombinase (HsRad51). With the aim of designing better inhibitors for cancer treatment, we combined an in silico docking approach with in vitro biochemical testing to construct a highly efficient chimera peptide from eight existing human BRC motifs. We built a molecular model of all BRC motifs complexed with HsRad51 based on the crystal structure of the BRC4 motif-HsRad51 complex, computed the interaction energy of each residue in each BRC motif, and selected the best amino acid residue at each binding position. This analysis enabled us to propose four amino acid substitutions in the BRC4 motif. Three of these increased the inhibitory effect in vitro, and this effect was found to be additive. We thus obtained a peptide that is about 10 times more efficient in inhibiting HsRad51−ssDNA complex formation than the original peptide.

Introduction

The human RAD51 protein (HsRad51[a]) is crucial for DNA repair processes that are based on homologous recombination between damaged loci and their undamaged copies in sister chromatids. The protein is thus involved in the repair of a double-stranded break, the most severe DNA damage.[1−4] Efficient DNA repair is usually beneficial for living organisms. However, in the case of cancer cells, their efficient DNA repair opposes the action of radio- and chemotherapies based on DNA damaging agents.[5−7] Rad51 is often overexpressed in cancer cells,[6−8] and its cellular amount is correlated in some way to resistance to anticancer treatment and to the degree of cancer advancement. Rad51 is thus a potential target for cancer treatment.

In fact, inhibiting the cellular expression of Rad51 directly by antisense or siRNA or indirectly by affecting the regulatory protein is found to slow down tumor development and increase survival time in mice besides increasing the efficiency of radio- and chemotherapies.[9−13] BRC motifs of human BRCA2 tumor suppressor, which are repeated eight times in the protein and are involved in the interaction with HsRad51,[14−16] are reported to inhibit the filament formation of HsRad51, the first step of the strand exchange reaction, in the cells and in vitro.[17−19] We have previously shown that even a small peptide of 28 amino acids derived from one of the BRC motifs (BRC4-28 peptide) can efficiently and selectively interact with HsRad51 and dissociate the HsRad51/single-stranded DNA (ssDNA) complex filament in vitro.[20] The peptide is thus a potential inhibitor of HsRad51 but unfortunately not efficient enough for medical use.

In this work, we have searched for an optimal amino acid sequence of the BRC peptide for the inhibition of Rad51 based on the existing eight BRC motifs of human BRCA2 protein. Various BRC motifs of different lengths (from 25 to 69 amino acids) have already been tested for their ability to bind to HsRad51.[16−19] All eight motifs were reported to bind to HsRad51.[16] However, only the structure of the HsRad51−BRC4 motif complex has been elucidated.[21] We therefore built molecular models of other BRC motifs by a homology strategy based on the crystal structure of the HsRad51−BRC4 motif complex. We then computed the interaction energy to HsRad51 of each residue in the different BRC motifs to find out which amino acid residue bound best at each of the binding positions of the peptide. The sequence thus proposed was then tested in vitro for its capacity to dissociate the HsRad51−DNA complex and inhibit the DNA strand exchange activity. The dissociation of the complex was monitored by measuring the fluorescence change of the poly(dA) analogue, poly(deoxy-1,*N*6-ethenoadenylic acid) (poly(dεA)) or the fluorescence anisotropy of fluorescein-labeled oligonucleotides, and by electron microscopy observation. The validity of the complex model was also tested by calorimetric analysis of HsRad51/peptide interactions.

Results

Search for the Minimum Size of an Active BRC4 Peptide. To design an optimal BRC peptide for the inhibition of HsRad51 recombinase, we searched for the best-binding amino acid sequence starting from that of the BRC4 peptide,

*To whom correspondence should be addressed. For M.T.: phone/fax, 33-2 5112 5636; E-mail, masayuki.takahashi@univ-nantes.fr. For A.S.: phone, 41-2 1692 4282; E-mail, Andrzej.Stasiak@unil.ch.

[a]Abbreviations: HsRad51, human RAD51 protein; ssDNA, single-stranded DNA; dsDNA, double-stranded DNA; poly(dεA), poly(deoxy-1,*N*6-ethenoadenylic acid); ITC, isothermal titration calorimetry.

 Published on Web 07/12/2010

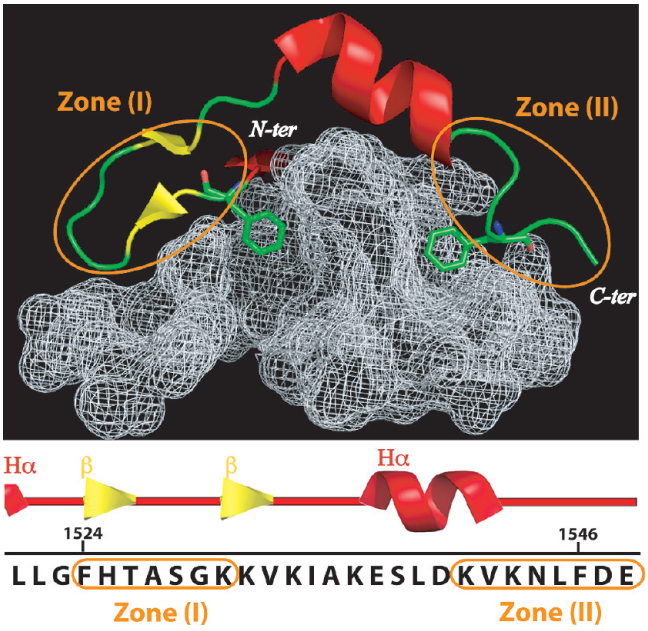

Figure 1. Interaction interface between the BRC4 peptide and HsRad51 protein. The BRC4 peptide (ribbon)/HsRad51 (mesh) interface is visualized from their complex structure.[21] The strong contact zones are noted in the 3-D structure and on the 28-amino acid sequence. The secondary structure of the peptide is indicated beside the sequence.

which we had previously studied with respect to its HsRad51-inhibition effect.[20] To alleviate the molecular modeling and biochemical analysis, we first searched for the minimum size of BRC4 peptide required for the inhibitory effect. Our previous study showed that separating the peptide into two parts, i.e., the β-hairpin N-terminal half and the α-helix C-terminal half, abolishes its ability to bind to HsRad51 and dissociate the HsRad51−DNA complex filament,[20] indicating that both parts are important for binding to HsRad51. However, we could not completely exclude the possibility that the central part of the peptide is also important for binding as its destruction by fragmentation abolishes the peptide activity.

The free energy of binding of the BRC4 motif to HsRad51 was therefore estimated by a further computational analysis. We computed the interaction energy (van der Waals short distance effect terms corrected by long distance Coulombic interactions) of each overlapping segment of eight amino acids of peptide instead of that of each amino acid residue to find out the zone(s) of peptide important for the binding to HsRad51. This computation was done on the crystal structure of the HsRad51−BRC4 motif complex. The analysis revealed two important zones: 1524-FHTASGK-1530 (zone I) at the N-terminal part and 1541-KVKNLFDE-1548 (zone II) at the C-terminal part (Figure 1). The results are compatible with a recent publication by Rajendra and Venkitaraman.[22] This indicates that the elimination of only a few amino acids from the C- or N-terminal part can destroy one of the contact zones and abolish the inhibitory effect of the peptide.

We tested the effect of deletions on the ability of peptides to dissociate the HsRad51−DNA complex by monitoring the fluorescence change of poly(dεA) as previously described[20] (Figure 2). The elimination of two amino acid residues from the N-terminal part (peptide BRC4−26), which conserves the binding zones, modified only slightly the dissociation capacity

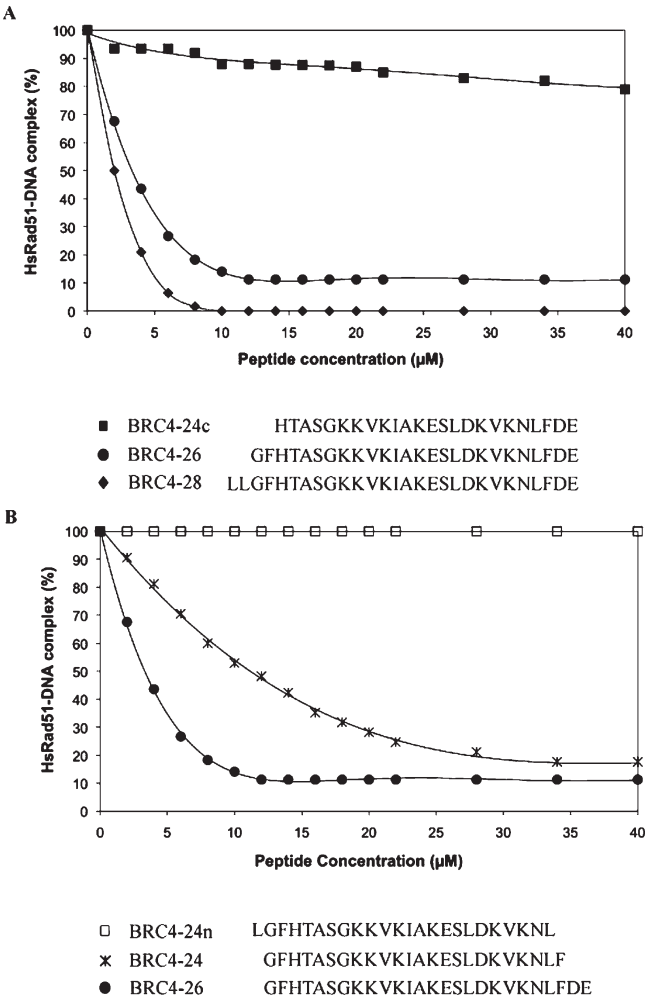

Figure 2. Effect of deletions in the N- and C-terminal parts of the BRC4 peptide on its capacity to dissociate the HsRad51−DNA complex. The dissociation of the HsRad51−ssDNA complex by N-terminal (A) and C-terminal deleted (B) BRC4-motif peptides was monitored by the decrease in fluorescence intensity of poly(dεA) upon stepwise addition of the peptides: BRC4-28 (closed diamonds), BRC4-26 (closed circles), BRC4-24c (closed squares), BRC4-24 (stars), and BRC4-24n (open squares). The amino acid sequence of peptides is noted under the figure to facilitate the visualization of the deleted parts. The experiments were performed using 1.5 μM HsRad51 and 3 μM (in bases) poly(dεA) in the presence of 1 mM ATP.

Table 1. Effect of Deletions of the BRC4 Peptide on Its Capacity to Dissociate the HsRad51−DNA Complex[a]

peptide	sequence	IC_{50} (μM)
BRC4-28	LLGFHTASGKKVKIAKESLDKVKNLFDE	2.1 ± 0.1
BRC4-26	GFHTASGKKVKIAKESLDKVKNLFDE	3.5 ± 0.2
BRC4-24c	HTASGKKVKIAKESLDKVKNLFDE	> 100.0
BRC4-24	GFHTASGKKVKIAKESLDKVKNLF	11.0 ± 0.3
BRC4-24n	FHTASGKKVKIAKESLDKVKNL	> 40.0

[a] IC_{50} was determined as the peptide concentration required for the half-dissociation of the HsRad51−poly(dεA) complex (1.5 μM HsRad51, 3 μM poly(dεA)) from Figure 2.

of the peptide. The concentration of this peptide required for the half-dissociation of the HsRad51−poly(dεA) complex was 3.5 μM compared to 2.2 μM for the original BRC4-28 peptide. In contrast, the deletion of two more residues (peptide BRC4-24c), which eliminates Phe1524 from binding zone I, strongly decreased the inhibitory capacity (Figure 2A, Table 1), underlining

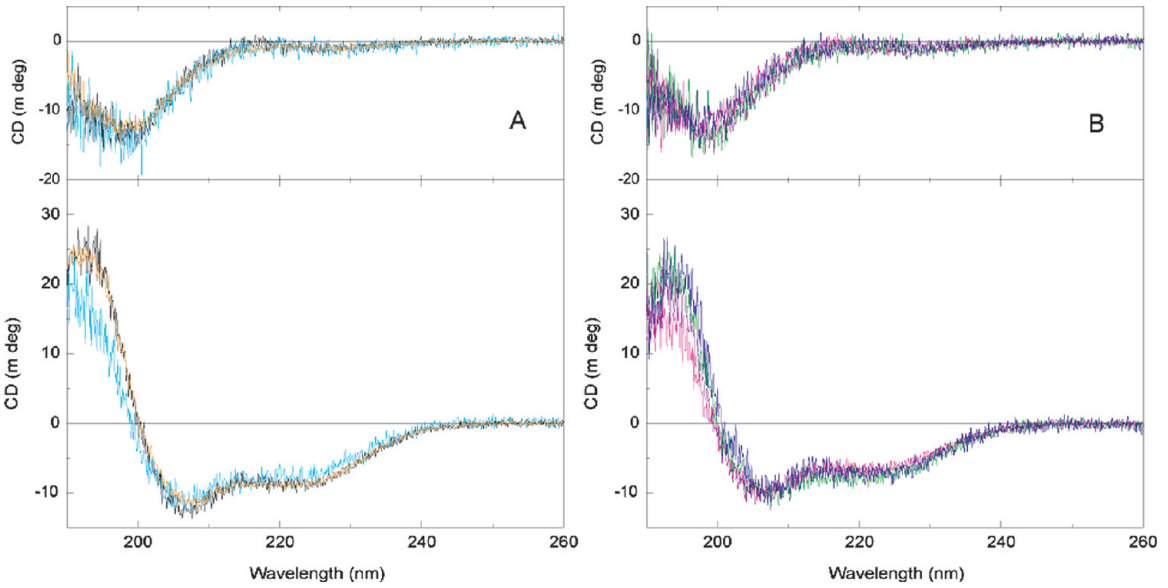

Figure 3. α-Helical folding potential of BRC peptides: CD analysis. CD spectra of 40 μM BRC peptides were measured in the presence (lower parts) and absence (upper parts) of 1 mM SDS. (A) CD of deleted peptides (BRC4-24, black; BRC4-24n, orange; BRC4-24c, cyan). (B) Substituted peptides (H/Y, magenta; A/S_1, olive; A/S_2, purple; L/F, navy).

the importance of zone I for the binding to HsRad51. This effect could be due either to the simple loss of interaction energy of Phe1524 or to the destabilization of the β-hairpin structure of zone I caused by the elimination of four amino acids. The first explanation seems more probable, although we could not completely exclude the second one because the substitution of Phe1524 by alanine without deletion of amino acids also abolishes the inhibitory effect (data not shown).

The elimination of two amino acid residues from the C-terminal of BRC4-26 (BRC4-24), which are in binding zone II, did not abolish the inhibitory effect but decreased it (Figure 2B). The half-dissociation of the complex was achieved with 11 μM peptide compared to 3.5 μM for the peptide that conserves this part (BRC4-26). The deletion of one more residue (BRC4-24n) completely abolished the inhibitory capacity (Figure 2B and Table 1), confirming the importance of zone II for the interaction with HsRad51. These deletions may not abolish the capacity of the peptide to form the α-helical structure because the peptide exhibited a CD signal corresponding to an α-helical structure in the hydrophobic environment (1 mM SDS) (Figure 3A) just like the original BRC4-28 peptide.[20] The effect of deletions is certainly a simple loss of contact with HsRad51 by the elimination of residues without a change in the binding conformation of the peptide. Supporting this idea, we observed that the substitution of Phe1546 by alanine also abolishes the inhibitory effect (data not shown).

Search for an Optimal BRC Sequence for HsRad51 Inhibition. We therefore decided to perform a sequence optimization on the 24-amino acid peptide (BRC4-24). To test systematically the effect of all possible substitutions (19 substitutions) of each residue on 24 positions is too time-consuming and unfeasible. We used an alternative strategy based on existing BRC-motif sequences: modeling all the BRC motifs based on the known BRC4 structure, taking the best residue (or segment) at different positions of the peptide and creating a chimera peptide by fusing them. All eight BRC motifs were reported to bind to HsRad51.[16] Therefore, all these motifs would be folded in a similar structure and interact with HsRad51 in the same way. This would permit us to use rather simple modeling approach to compute the interaction energy (see Discussion).

We first searched in the data bank using the BLAST program for protein segments that are similar in sequence to the BRC4 motif. All sequences found were consistently related to the BRC motifs of mammalian BRCA2 proteins. We therefore tested only the BRC motifs of human BRCA2 protein (Figure 4A). Because the structure of only the BRC4 motif is known, we built a 3-D model of seven other BRC motifs by a homology approach based on the structure of the BRC4 motif in the complex with HsRad51 after sequence alignment (Figure 4A). We then positioned these folded peptides in the place of the BRC4 motif to build a model of other BRC motif−HsRad51 complexes. BRC4 appears to be a good template in that we did not find any major steric clashes between any peptide and HsRad51. All constructions were further refined by energy minimization, first optimizing the side chain orientation of the peptide and HsRad51, then the side chain and backbone of the peptide, and finally both the backbone structure of HsRad51 and that of the side chains, as described in the Experimental Section.

On the basis of the complex models thus built, we computed the intermolecular interaction energy of each residue of each BRC motif for HsRad51 binding. We then compared the interaction energies of various peptides at a given binding position (Figure 4B). At almost all the positions, the residues of the BRC4 motif exhibited the best interaction energy (data not shown), in accord with the observation that BRC4 has the best affinity for HsRad51 among the BRC motifs.[18] However, at four positions, other residues exhibited a better interaction energy than those of the BRC4 motif: Tyr in the place of His at 1525, Ser in the place of Ala at 1527 and 1535, Phe and Trp in the place of Leu at 1545 (Figure 4B). We then examined the effect of these substitutions in the BRC4 motif, one by one, on the HsRad51 binding by rebuilding the complex model and recalculating the interaction energy. As expected from our assumption of an independent energy contribution of each residue, in all cases except one, our

A

BRC1	1007 - G G S F R T A S N K E I K L S E H N I K K S K M F F K D - 1034	
BRC2	1216 - F R G F Y S A H G T K L N V S T E A L Q K A V K L F S D - 1243	
BRC3	1425 - D T F F Q T A S G K N I S V A K E S F N K I V N F F D Q - 1452	
BRC4	1521 - L L G F H T A S G K K V K I A K E S L D K V K N L F D E - 1548	
BRC5	1668 - A L A F Y T S C S R K T S V S Q T Q L L E A K K W L R E - 1695	
BRC6	1841 - P P A F R I A S G K I V C V S H E T I K K V K D I F T D - 1868	
BRC7	1975 - C G I F S T A S G K S V Q V S D A S L Q N A R Q V F S E - 2002	
BRC8	2055 - F S G F S T A S G K Q V S I L E S S L H K V K G V L E E - 2082	

B

BRC4 Position	BRC3		BRC4		BRC5		BRC6	
	Residue	Ei (Kcal/mol)	Residue	Ei (Kcal/mol)	Residue	Ei (Kcal/mol)	Residue	Ei (Kcal/mol)
1525	Q	-6.77	H	-5.35	**Y**	**-8.06**	R	-4.16
1527	A	-6.26	A	-1.23	**S**	**-7.52**	A	-5.11
1535	A	-8.71	A	-9.60	S	-11.75	**S**	**-21.37**
1545	**F**	**-9.71**	L	-6.79	**W**	**-11.84**	L	-4.53

C

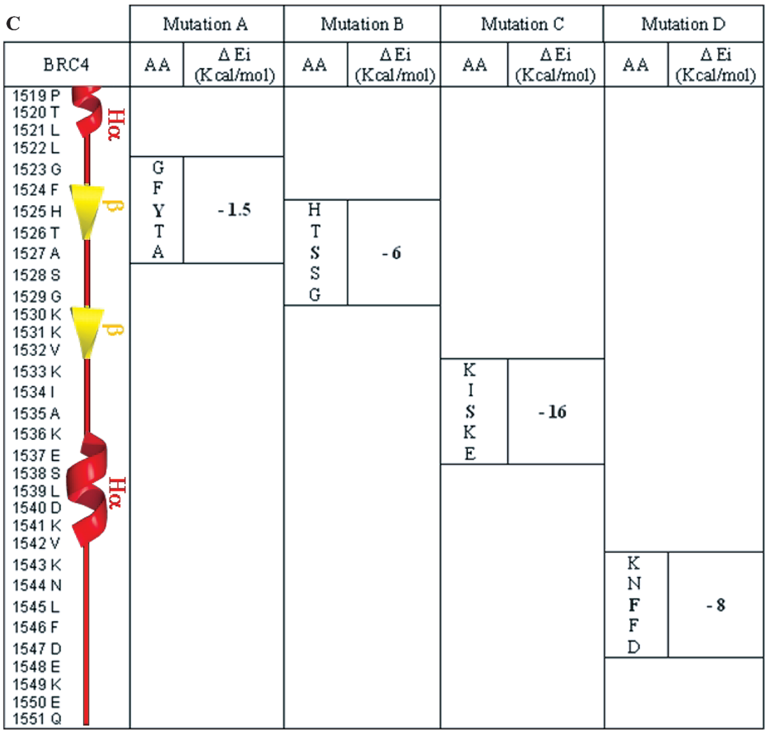

Figure 4. Proposition of amino acid substitutions of the BRC4 peptide to gain in interaction energy by comparison with the interaction of other BRC motifs with HsRad51. In (A), the amino acid sequences of the eight human BRC motifs are aligned and the best residues in interaction energy to HsRad51 at the given position are colored. In (B), the interaction energy of residues of different BRC motifs at given positions is shown. In (C), relative local energetic gain (ΔEi) is calculated for each substitution. The secondary structure of the BRC4 motif is presented at the left side to facilitate the identification of substitution positions.

calculations revealed a significant increase in interaction energy related to a better affinity of the BRC motif toward HsRad51 (Figure 4C).

The only exception (Leu1545Trp) was analyzed by comparing the source and target contexts (BRC5 and BRC4, respectively). Graphical display showed that the tryptophan residue substituting Leu1545 could not penetrate into a cavity of HsRad51 mainly because of the neighboring bulky Phe1546 residue. In contrast, in BRC5, the sequence corresponding to Leu(1545)-Phe(1546) of BRC4 is Trp-Leu. Therefore, in this local but essential restricted zone of BRC/HsRad51, each initial sequence (Trp-Leu for BRC5 and Leu-Phe BRC4) is sterically acceptable but not the combination Trp-Phe derived from our protocol. The cavity, however, can accommodate two phenylalanine residues (Figure 5B), and thus the substitution of Leu1545 by Phe can increase the interaction energy. Graphical display also showed that the substitution of Ala at 1535 by Ser creates a hydrogen bonding (Figure 5A) and may thus enhance the binding. Concerning the substitutions of His at 1525 by Tyr and Ala at 1527 by Ser, we could not visualize the reason for the binding enhancement.

Validation of Peptide Modeling: Effect of Sequence Modifications on the Inhibition of HsRad51−DNA Complex Formation and the Strand Exchange Reaction. We first tested the validity of our modeling by calorimetric analysis of HsRad51/peptide interactions, then by measuring the BRC peptide-promoted dissociation of the HsRad51−DNA complex, and finally by evaluating the inhibition of the strand exchange reaction. We also verified our assumption, using

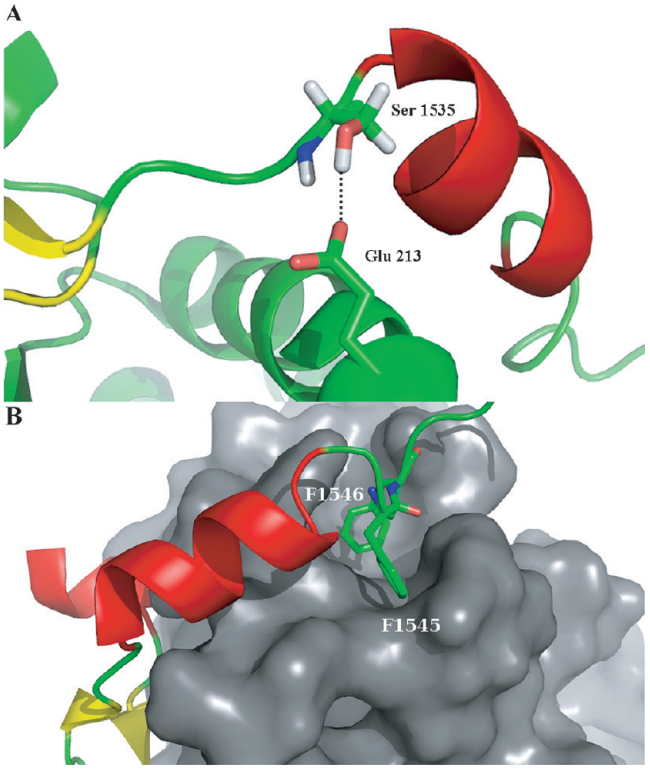

Figure 5. Effect of amino acid substitutions on the contact with HsRad51. (A) Substitution of Ala1535 by serine creates a new hydrogen bonding with Glu213 of HsRad51. (B) Substitution of L1545 by phenylalanine strengthens the interaction with a hydrophobic pocket of HsRad51 (gray surface).

CD measurements, that the sequence modifications did not affect the potential folding pattern of the peptides. All the peptides exhibited a CD spectrum corresponding to a nonstructured state in aqueous solution (Figure 3B). However, the spectrum was modified upon addition of 1 mM SDS, which mimics a hydrophobic environment, thus indicating the formation of an α-helical structure just as for the original BRC4 peptide. These peptides can be partially folded in an α-helical structure for interaction with HsRad51 as observed for the BRC4 motif.[21]

The isothermal titration calorimeter (ITC) directly measures the enthalpy of interaction and also enables the determination of the binding constant and entropy.[23,24] This measurement is thus a useful tool to verify the binding model. We performed the ITC measurements of the binding of these peptides to HsRad51 and compared them with the result for the original peptide of the same size (BRC4-24) (Typical titration is shown in Supporting Information Figure S1). The measurements were made using mutated monomeric HsRad51 (HsRad51−F86E) instead of wild type HsRad51 because the binding of BRC peptides dissociates HsRad51 oligomers and the ITC measurements would provide the sum of the binding energy of peptide to HsRad51 and the dissociation energy of HsRad51 oligomers. Using monomeric HsRad51 enables the binding energy of peptides to HsRad51 to be measured selectively. The absence of oligomerization of HsRad51−F86E was verified by molecular sieve chromatography of the protein under the ITC measurement conditions (data not shown). The results of the ITC measurements were analyzed according to a one-binding-site model and nicely fitted for all the cases with a binding

Table 2. Calorimetric Analysis of HsRad51/Peptide Interactions[a]

peptide	K (10^5 M^{-1})	ΔH (kcal/mol)	$\Delta(\Delta H)$ (kcal/mol)	ΔS (cal/mol/deg)	$\Delta(\Delta S)$ (cal/mol/deg)
BRC4-24	1.4 ± 0.4	−12.3 ± 1.6		−18	
H/Y	3.8 ± 2.8	−14.1 ± 2.5	−1.5	−20	−2
A/S_1	< 0.1	nd	nd	nd	nd
A/S_2	5.2 ± 1.5	−14.3 ± 2.6	−2.0	−21	−3
L/F	7.3 ± 4.3	−11.5 ± 2.5	+0.8	−14	+4

[a] nd: not determined.

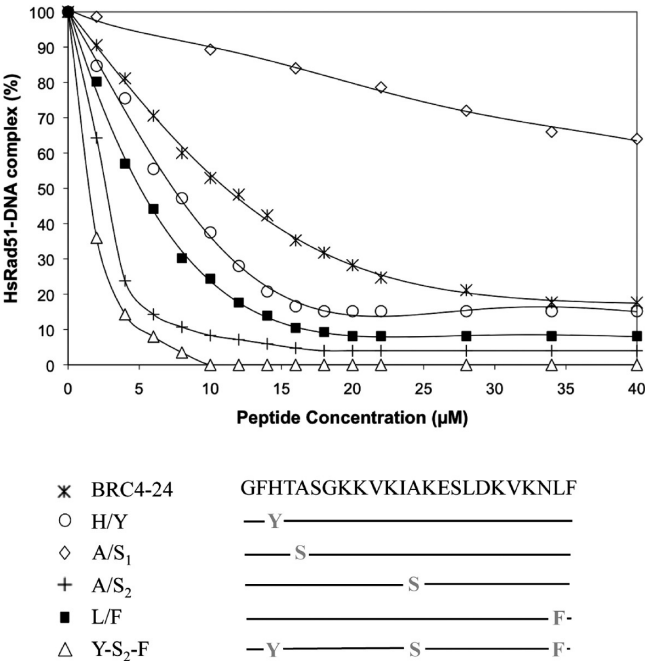

Figure 6. Effect of amino acid substitutions of the peptide on its capacity to dissociate the HsRad51−DNA complex. The dissociation of the HsRad51−ssDNA complex by modified BRC4-motif peptides was monitored by the decrease in fluorescence intensity of poly(dεA) upon stepwise addition of the peptides as in Figure 2. Open diamonds, A/S_1 (Ala1535Ser); open circles, H/Y (His1525Tyr); closed squares, L/F (Leu1545Phe); crosses, A/S_2 (Ala1535Ser); open triangles, Y-S_2-F peptide with three amino acid substitutions.

stoichiometry of about 1 (1.1 ± 0.1 peptide−HsRad51 monomer). The analysis was thus self-consistent. Furthermore, the analysis with a model of two binding sites did not provide good fitting.

The binding parameters thus obtained support our prediction concerning the substitutions of His1525Tyr (H/Y), Ala1535Ser (A/S_2), and Leu1545Phe (L/F): all these substitutions increased the binding affinity of peptide to HsRad51 (Table 2). Furthermore, in the case of Leu1545Phe substitution, the ITC measurements showed enhancement in the reaction entropy ($\Delta(\Delta S)$ positive) without significantly changing ΔH. This is in accord with the modeled complex (Figure 5B), in which the hydrophobic interaction is enhanced and thus the entropy of interaction should be increased. Good accord between the experimental data and the model was observed also for Ala1535Ser substitution (A/S_2 peptide). The visualization of complex shows creation of an extra hydrogen bond and predicts improvement in enthalpy of interaction. The ITC measurements shows that the Ala1535Ser (A/S_2) substitution enhanced the enthalpy ($\Delta(\Delta H)$ negative) slightly disfavoring the entropy of reaction (Table 2).

Table 3. Effect of Amino Acid Substitutions of the BRC4 Peptide on Its Capacity to Dissociate the HsRad51−DNA Complex[a]

peptide	sequence	poly(dεA) IC_{50} (μM)	oligo$(AGT)_{12}$ IC_{50} (μM)	K_i (μM)
BRC4-24	GFHTASGKKVKIAKESLDKVKNLF	11.0 ± 0.3	6.00 ± 0.03	10.0
H/Y	GFYTASGKKVKIAKESLDKVKNLF	7.0 ± 0.3	2.70 ± 0.02	6.0
A/S_1	GFHTSSGKKVKIAKESLDKVKNLF	> 40		> 40.0
A/S_2	GFHTASGKKVKISKESLDKVKNLF	2.5 ± 0.1	2.00 ± 0.02	1.8
L/F	GFHTASGKKVKIAKESLDKVKNFF	5.0 ± 0.2	2.60 ± 0.02	4.2
$Y\text{-}S_2\text{-}F$	GFYTASGKKVKISKESLDKVKNFF	1.5 ± 0.1	1.05 ± 0.01	0.75

[a] IC_{50} was determined as in Table 1 and apparent K_i as the concentration of free peptide at half-dissociation.

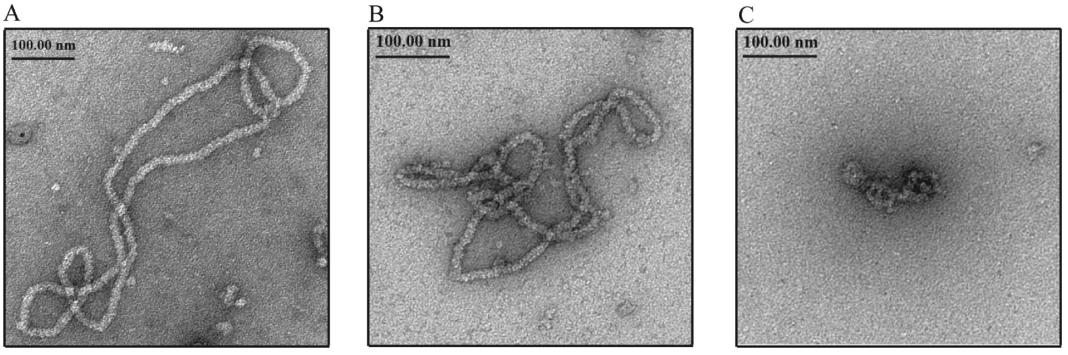

Figure 7. Electron microscopy observation of the effect of $Y\text{-}S_2\text{-}F$ BRC peptide on the HsRad51−ssDNA complexes. HsRad51−ssDNA filaments formed between HsRad51 (5 μM) and ΦX174 ssDNA (10 μM in bases) were observed by electron microscopy after addition of 10 μM (B) or 50 μM (C) $Y\text{-}S_2\text{-}F$ BRC peptide or without peptide (A).

In contrast to these peptides, we did not observe any significant heat change upon injection of peptide, in which Ala at 1527 is substituted by Ser (A/S1 peptide). There may be no significant interaction, i.e., decrease in the binding affinity by this substitution. The residue is situated in the β-turn structure (Figure 4C), and thus the substitution may decrease the stability of this active conformation and, consequently, the capacity to bind to the HsRad51.

We then tested the capacity of these peptides to cause dissociation of the HsRad51−ssDNA complex. The dissociation capacity was first monitored by the decrease in fluorescence intensity of poly(dεA), a fluorescent etheno analogue of poly(dA) (see the Experimental Section). All the substitutions, except that of Ala at 1527 by Ser (A/S_1 peptide), were found to increase the dissociation capacity of the peptide: lower concentrations of peptide were sufficient to cause dissociation of the HsRad51−poly(dεA) complex (Figure 6). The concentrations of peptide required for half-dissociation decreased from 11 μM (BRC4-24) to 7 μM for His1525Tyr (H/Y peptide), to 2.5 μM for Ala1535Ser (A/S_2 peptide) and to 5 μM for Leu1545Phe (L/F peptide) substitutions (Table 3). The effect was rather additive: the peptide in which the three residues were substituted ($Y\text{-}S_2\text{-}F$ peptide) exhibited better efficiency and the half-dissociation occurred at 1.5 μM. The apparent K_i was estimated using the formula ($K_i = [\text{peptide}]_{total} - [\text{HsRad51}]/2$), with the assumption that the binding stoichiometry of peptide to HsRad51 is 1 per monomer as indicated by the ITC measurements (see Supporting Information). We observed that the K_i of the peptide with the three substitutions became less than 1/10 of that of the original peptide (Table 3). We obtained similar results using the fluorescein-labeled oligo$(AGT)_{12}$ oligonucleotide (Table 3), showing that the increase in the dissociation activity is independent of DNA sequence as expected.

The action of the modified peptide on the preformed HsRad51−ssDNA complexes was further verified by electron microscopy observations of complexes formed with ΦX174 ssDNA (Figure 7). In the absence of the peptide, we observed regularly structured extended HsRad51−ssDNA filaments as reported earlier for these types of complexes[25,26] (Figure 7A). When 10 μM of $Y\text{-}S_2\text{-}F$ BRC peptide was added to the preformed HsRad51−ssDNA complexes, the filaments lost their regularity and revealed the presence of kinks, presumably corresponding to points where HsRad51 started to depolymerise and dissociate from ssDNA (Figure 7B). At a still higher concentration of $Y\text{-}S_2\text{-}F$ BRC peptide (50 μM), the preformed HsRad51−ssDNA complexes almost completely dissociated (Figure 7C). Thus, we have demonstrated by EM that the peptide can dissociate even large HsRad51−ssDNA complexes and have confirmed the results of assays based on fluorescence measurements.

In contrast to these substitutions, the substitution of Ala at 1527 by Ser (A/S1) decreased the efficiency: the half-dissociation required more than 40 μM peptide (Figure 6, Table 3). The substituted peptide may not bind efficiently to HsRad51, as indicated by the ITC measurements (Table 2), and could not dissociate the Rad51−DNA complex.

Finally, we tested the inhibitory effect of peptides on the DNA strand exchange activity of HsRad51. The strand exchange reaction between a short single-stranded oligonucleotide and a double-stranded oligonucleotide of the same sequence was performed in the presence of various concentrations of peptides. As expected, the strand exchange reaction was more efficiently inhibited by substituted peptides (Figure 8) corresponding well to the increase in the ability to promote the dissociation of the HsRad51−DNA complex.

Discussion

On the basis of the relevant starting point for HsRad51 inhibition (crystallographic data of the complex formed with the BRC4 motif), our goal was to design more efficient BRC-motif peptides. The prediction of ligand binding affinity is one of the most challenging applications of computational

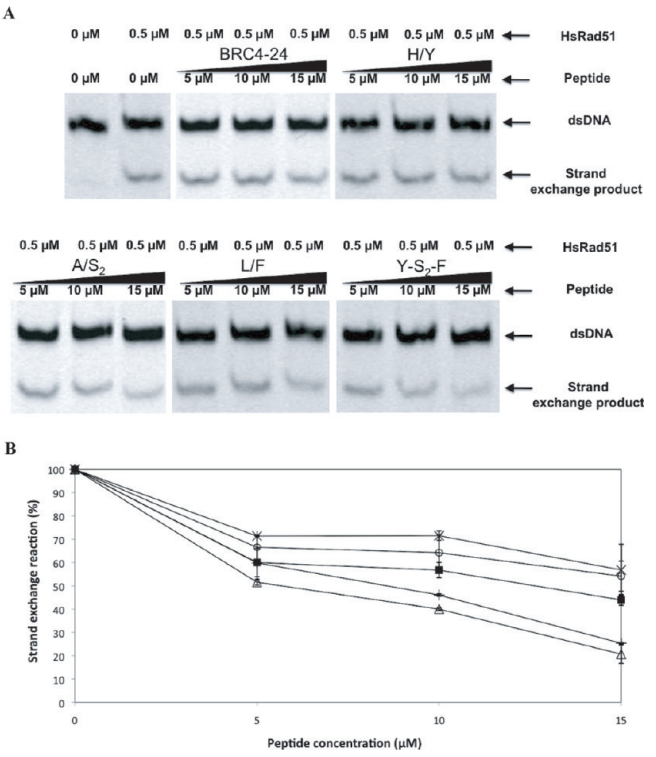

Figure 8. Inhibition of the DNA strand exchange reaction by the modified BRC4 peptides. The HsRad51-promoted (0.5 μM) strand exchange reaction between single-stranded and double-stranded oligonucleotides in the presence of indicated concentrations of BRC4 peptides was analyzed by quantifying the reaction product (B) after its separation by polyacrylamide gel electrophoresis (A) as described in the Experimental Section. Stars, BRC4-24; circles, H/Y; squares, L/F; crosses, A/S2; triangles, Y-S2-F peptides.

chemistry. Ultimately, ranking compounds according to their estimated affinities to a given molecule by means of molecular mechanics scheme is of particular interest for structure-based drug design. From a theoretical point of view, free energy is the potent value to estimate binding constants and corresponding calculations have hugely progressed because of the improvement of force fields and development of numerical algorithms and protocols in conjunction with considerable progress in computer power. Assuming that a set of experimental binding data is available, reproducing them by computational methods could be done by numerous protocols mainly depending on the expected accuracy and theoretical complexity.

To one extremity, the simplest way is to use empirical or statistical multivariate equations (QSAR). A scoring function is a simple estimation of relative binding affinities for virtual screening methods mainly based on shape and chemical complementarity. At the other extremity, most rigorous methods to get access to the ligand−receptor binding enthalpy are quantum mechanics (QM) calculation or at least a combination of quantum mechanics and molecular mechanics (QM/MM). But so far, these approaches are excessively expensive in term of engaged computational resources. In addition, solvent effects are not always well taken into account and, usually, an appropriate treatment would require implicit solvent models where water is assimilated to a continuum dielectric medium. This approximation yielded to solvation free energies with two protocols: Poisson−Boltzmann/surface area (MM-PBSA) and generalized Born/surface area (MM-GBSA). Thus, the exploration of the conformational space will be achieved by very long MD simulations to determine equilibrium averages with methods of free-energy perturbation (FEP) or thermodynamic integration (TI).

With an intermediate accuracy, classical molecular mechanics (MM) approaches appear as a good balance between computer time and energy accuracy for large molecular systems by taking into account both induced fit of all molecular partners. Thus free energy calculations can be achieved by different ways depending on approximations used. Basically, most force fields employed these two last decades are expressed as the sum of independent terms of bonded and nonbonded interactions, whatever the mathematical expression of each term is. Bonded interactions are based on internal parameters of molecules covalently described (bonds, angles, and dihedrals), and obviously these terms do not participate to the affinity between molecules. Nonbonded interactions mainly include van der Waals short distance effect terms (generally expressed by a repulsive−attractive Lennard-Jones 6−12 potential) corrected by long distance Coulombic interactions (between point charges centered on each atom). When applied to atoms of the same molecule, these two types of interactions participate to its potential energy. Conversely, calculated between atoms of two different molecules, the sum of these nonbonded interactions is defined as interaction energy by most softwares (Discover, CHARMM, ...).

This term is the energy criterion used here. Practically, when calculations are done for a series of ligands (similar in shape and chemical properties) interacting with the same target molecule, these interaction energies could be qualitatively assimilated to relative binding affinities if each ligand−target complex minimized is the most probable docking solution. Furthermore, this simple scheme does not take into account the role of explicit water molecules capable to significantly modify the affinity between two molecules measured in vacuum. For these reasons, we chose a relatively simple modeling approach based on interaction energies and checked how good it is as a predictive tool to in silico reveal potential oligopeptide leads prior to any biochemical syntheses and further in vitro activity tests. Finally, we considered that interaction energy values already successfully used in several previous papers[27−29] were adequate with regards to the modeling construction scheme (basically by homology to initial BRC4-28 peptide, no water molecule taken into account).

For this purpose, we took advantage of all the biological data available. An initial search for BRC4 sequence similarity using the BLAST algorithm yielded exclusively BRC motifs of mammalian BRCA2 proteins. This strengthens the possible functional specificity of these motifs, at least for HsRad51 interaction. The 3-D folding of BRC4 observed in the crystallographic complex was used as a pattern to model all other BRC motifs in complex with HsRad51. Because of the geometrical features of the pattern, we could assume additivity of local binding energies. This enabled us to design an optimal peptide by selecting the best amino acid residue (or segment) at a given binding position and fusing them as a chimera peptide. We have thus gained a 10 times more efficient peptide by combining the eight existing human BRC motifs. This approach alleviates the model building compared to the systematic substitution of amino acids in the peptide. Furthermore, it can potentially replace a segment of the peptide while the systematic substitution approach allows only one amino acid residue to be changed at a time. The approach could also avoid unexpected conformational change of peptide upon amino acid substitution. The method

is thus interesting and could be applied to other systems in which the interacting segment is repeated or a protein family is involved.

The observation that 3 of our 4 propositions are experimentally confirmed supports our assumption that all BRC motifs of BRCA2 bind to HsRad51 in the same conformation. The unexpected effect of the Ala1527Ser substitution, i.e., the decrease in inhibitory effect, may, in contrast, be due to destabilization of the β-turn organization at the N-terminal part, in which Ala1527 is situated. Further analysis is in progress to examine this explanation by more vigorous model building including the dynamics and also by NMR measurements. Except for this part, the motifs bind in a rather extended form and each residue interacts with HsRad51 roughly independently of its neighboring residues. This is supported by the observation that the increase in efficiency by substitution is rather additive. Our model building is also supported by ITC calorimetric measurements: as expected, Leu1545Phe substitution improves the entropy contribution and Ala1535Ser substitution enhances the enthalpy.

These observations suggest that stabilization of the active conformation would further increase the efficiency of the peptide. The peptide is not structured in free form in solution according to the CD measurements while it should be organized in β-turn and α-helix to bind to HsRad51 (Figure 3), as observed in the crystal structure of the complex.[21] Formation or stabilization of the active form before binding to HsRad51 certainly facilitates the interaction and enhances the inhibitory effect. In accord with this concept, the ITC calorimetric analysis showed that the binding of peptide to HsRad51 is disfavored by entropy (ΔS negative), suggesting that one part of the binding energy is used for the organization of the peptide from random coil. The importance of α-helix was suggested by our recent observation that the some substitutions, which should not affect the interaction with HsRad51 but disfavors α-helix formation, inhibits the in vitro strand exchange reaction less efficiently.

It has been reported recently that in vitro binding of HsRad51 to ssDNA was promoted by BRC motifs supplied either in a form of BrcA2 domain containing the eight BRC repeats or in a form of 35 amino acid peptide.[30,31] The same authors observed however that formation of HsRad51−dsDNA complexes was inhibited by the addition of BRC motifs and that both of the effects resulted in a stimulation of HsRAD51-mediated strand exchange reaction. We were especially concerned by the reported stimulation of HsRad51 recombination by the short peptide of 35 amino acids because this of course would compromise our plan to use peptides with BRC repeats as inhibitors of HsRad51-mediated DNA repair by homologous recombination.[30] However, the peptides used by us did not show stabilization of HsRad51−ssDNA complexes even at low peptide concentration. This applied not only to complexes formed with synthetic oligonucleotides but also to complexes formed with long ΦX174 ssDNA molecules with natural base sequence. We think that the fact that our peptides were shorter than these used by Carreira et al.[30] is likely the cause of the difference. A very recent work by Rajendra and Venkitaraman showed the importance of LFDE sequence at the C-terminal of BRC4 motif for binding to HsRad51 and concluded that this motif stimulates HsRad51 oligomerization.[22] In the case of 35 amino acids peptide studied by Carreira et al., the LFDE sequence was still followed by additional three amino acids, which permitted this motif to be in its natural environment. Our peptides that range from 24 to 28 amino acids have a shorter C-terminal and either miss the DE residues completely or terminate just after LFDE motif, which apparently interferes with possible stimulatory action of LFDE sequence on the formation of HsRad51−ssDNA complexes. According to Rajendra and Venkitaraman the inhibitory module of each repeat is positioned close to N-terminal of 35 amino acid BRC repeat. This module has the sequence FxxA and all our peptides that showed destabilizing action on HsRad51 complexes contained this entire sequence and was still flanked by at least one amino acid toward the N-terminal. Therefore, our results are fully consistent with these by Rajendra and Venkitaraman and show that BRC repeat fragments containing only fully functional inhibitory modules with the FxxA sequence can be used for specific inhibitions of HsRad51-medited homologous recombination. With further improvements, such peptides may become efficient enough for use at the cellular level and could become a promising candidate for the design of anticancer drugs.

Conclusions

Taking advantage of the reported crystal structure of BRC motif−Rad51 complex, we designed more efficient chimera peptide from the existing eight human BRC motifs with the help of a rather simple in silico docking approach and verified its efficiency by in vitro biochemical testing.

Experimental Section

Modeling Methods. The atomic coordinates of the BRC4 peptide−HsRad51 complex were taken from the 3-D structure determined by X-ray crystallography at 1.7 Å resolution[21] (Protein Data Bank access no. 1N0W). Amino acid sequences similar to BRC4 were searched for in the SwissProt data bank. The sequence alignment was carried out using the Blast program accessible at Pôle Bioinformatique Lyonnais (http://pbil.univ-lyon1.fr). Visualization of the complex and interaction energy calculations were performed with the InsightII Accelrys software[32] under the CFF91 force field[33,34] and using a steepest descent algorithm. Intermolecular binding energies between each amino acid residue of the BRC peptides and HsRad51 were estimated using the DOCKING option, taking into account the electrostatic and van der Waals nonbounded energies. Intermolecular binding energies between the segments of 7/8 amino acids of the BRC peptides and HsRad51 were also computed in the same manner.

Model building of various BRC motifs in complex with HsRad51 was based on the crystal structure of the BRC4 peptide−HsRad51 complex:[21] after sequence alignment, each peptide was folded and positioned to HsRad51 on the basis of the BRC4 peptide backbone. From these initial constructions, only a few changes in the orientation of the peptide side chains or HsRad51 residues were necessary to avoid local steric conflict. Next, the complex structures were refined by 20000 cycles of minimization, keeping their backbone structure as observed in the crystal structure. A supplemental step of 20000 cycles of minimization without any constraints on the BRC peptides but keeping the backbone structure of HsRad51 was performed to monitor the adaptation and the relaxation of BRC peptides in the HsRad51 complex context. Finally, 20000 cycles of minimization were performed without any constraints.

Protein Preparation. Wild type HsRad51 and HsRad51−F86E, which cannot form polymers,[21] were prepared as described in Nomme et al.:[20] the N-terminal hexahistidine-tagged HsRad51 were expressed in the JM109(DE3) strain of *Escherichia coli* that also carries an expression vector for the minor tRNAs (Codon(+)RIL, Novagen), and purified on nickel-nitrilotriacetic

acid (Ni-NTA) agarose (Invitrogen). HsRad51−F86E was eluted with a linear gradient of 10−60 mM imidazole while wild type HsRad51 was eluted with a gradient of 60−500 mM imidazole. The hexahistidine tag was then removed from the HsRad51 portion with thrombin (Amersham Biosciences), and the proteins were further purified by chromatography on a MonoQ column (Healthcare Biosciences). Protein concentrations were determined using the Bio-Rad protein assay kit with bovine serum albumin (Pierce) as a standard protein.

Peptides. The peptides spanning the part of the BRC4 motif of BRCA2 protein were prepared by Neosystem (France): BRC4-28 (1521−1548), BRC4-26 (1523−1548), BRC4-24 (1523−1546), BRC4-24c (1525−1548), BRC4-24n (1522−1545). The amino acid composition and purity of the peptides were verified by mass spectroscopy and HPLC analysis (Supporting Information Figure S2). The purity of all the peptides except BRC4-28 (94%), H/Y (94%), and Y-S_2-F (94%) was more than 95%. All modified BRC4-24 peptides, in which one or more residues were replaced with another, were synthesized by the Fmoc solid-phase method using the ABI433A peptide synthesizer (PE Applied Biosystems, USA). The peptides were deprotected at the side chains and liberated from the resin by reaction with Reagent K (9 mL of trifluoroacetic acid (TFA), 0.5 mL of water, 0.5 mL of phenol, 0.5 mL of thioanisole, and 0.25 mL of ethanedithiol) for 3 h at room temperature. The crude peptides were purified by reversed-phase high performance liquid chromatography (RP-HPLC) on a C8 column (VYDAC, USA) and eluted with a linear gradient of 0.05% TFA and acetonitrile (Supporting Information Figure S3). Molecular weights were confirmed by MALDI-TOF mass spectrometry on Voyager DE-PRO (PerSeptive Biosystems, USA). The N-terminal of all the peptides was acylated.

Dissociation of HsRad51−DNA Complex Filament. The BRC peptide-promoted dissociation of the HsRad51−single-stranded DNA (ssDNA) complex filament was monitored by the change in fluorescence of poly(dεA), the poly(dA) analogue, and the change in fluorescence anisotropy of fluorescein-labeled oligonucleotide (oligo(AGT)$_{12}$) (Genset, France).[35] Poly(dεA) was prepared by chemical modification of poly(dA) (Pharmacia), as described in ref 36, and its fluorescence was measured at 410 nm (bandwidth: 5 nm) with excitation at 320 nm (bandwidth: 3 nm) in an FP-6500 spectrofluorimeter (Jasco, Japan). The fluorescence anisotropy was measured in a J-715 fluorescence polarimeter (Jasco, Japan) averaging over 20 measurements. Most experiments were performed at 25 °C in 20 mM (in phosphate) sodium phosphate buffer, pH 7.4 containing 50 mM NaCl, 1 mM $MgCl_2$, and 1 mM ATP. The buffer was filtered on a nitrocellulose filter (pore size: 0.2 μm) (Pall Corporation, USA) and degassed. The concentration of HsRad51 was 1.5 μM and that of poly(dεA) was 3 μM in bases for poly(dεA) experiments, and 0.5 μM of HsRad51 and 1 μM in bases of oligo(AGT)$_{12}$ for the anisotropy experiments.

Electron Microscopy. The BRC peptide-promoted dissociation of HsRad51−ssDNA complexes was also monitored by electron microscopy. The HsRad51−ssDNA complex was formed by incubation of circular ΦX174 ssDNA (10 μM in bases) with HsRaD51 (5 μM) in a 20 mM (in phosphate) sodium phosphate buffer, pH 7.4 containing 1 mM $MgCl_2$ and 5 mM ATP for 15 min at 37 °C. BRC peptide was then added at the indicated concentrations. After a further 15 min of incubation, glutaraldehyde was added to the final concentration of 0.1% to fix protein−DNA complexes. The fixation was performed for 15 min at 37 °C. Samples of the reactions were then diluted 10-fold in 5 mM magnesium acetate and used for adsorption onto glow-discharged, carbon-coated electron microscopy grids. After negative staining in 2% uranyl acetate,[37] the images of samples were recorded at a magnification of 22000 using a Philips CM12 electron microscope.

Strand Exchange Assay. The DNA strand exchange reaction between 58-mer ssDNA and the IRD-labeled homologous 32-mer double-stranded DNA was performed as previously described.[20] Then 0.5 μM of HsRad51 in the presence of indicated concentrations of BRC4 peptides was incubated with a 58-mer ssDNA (100 nM in fragment) in 10 μL of standard reaction buffer containing 20 mM Tris-HCl (pH 8.0), 1 mM ATP, 1 mM DTT, 100 μg/mL BSA, 20 mM $MgCl_2$, 2 mM creatine phosphate, 75 μg/mL creatine kinase, and 2% glycerol, at 37 °C for 20 min. The reaction was initiated by adding the 32-mer dsDNA (10 nM in fragment). After 1 h of incubation at 37 °C, the reactions were stopped by the addition of 0.7% SDS and 0.7 mg/mL proteinase K (Roche Molecular Biochemicals). The reaction mixtures were further incubated for 10 min at 37 °C. After addition of loading dye, the reaction products were subjected to electrophoresis on 15% polyacrylamide gel. The electrophoresis was carried out with TBE buffer (90 mM Tris, 90 mM boric acid and 2 mM EDTA) and applying 10 V/cm for 3 h. The products were visualized by detection of IRD-800.

CD Measurements. CD signals of peptides were measured in a J-810 CD spectrometer (Jasco, Japan) equipped with a Peltier effect temperature controller and using a 1 cm × 0.2 cm quartz cell with four windows (Hellema, Germany), allowing measurement with either a 1 or 0.2 cm path length. The CD spectra were measured from 260 to 190 nm in step mode (bandwidth: 2 nm; interval: 0.1 nm; response time: 0.125 s; path length: 0.2 cm; temperature: 20 °C) and averaged over two scans to increase the signal-to-noise ratio. The variation in the CD signal at 220 nm with rising temperature was measured (bandwidth: 10 nm, interval: 0.1 C; response time: 1 s, path length: 1 cm) by increasing the temperature from 20 to 85 °C at a rate of 1 °C/min. All the CD experiments were performed with 45 μM peptide in 20 mM (in phosphate) sodium phosphate, pH 6.8.

Isothermal Titration Calorimetry (ITC) Measurements. ITC measurements for the binding of BRC peptides to monomeric HsRad51 (HsRad51−F86E) were performed in a Microcal V200 ITC apparatus (filtering time: 2 s; injection interval: 120 s; syringe rotation: 1000 rpm) at 25 °C. The buffer was 20 mM (in phosphate) sodium phosphate, pH 7.4 with 50 mM NaCl, 1 mM $MgCl_2$, and the protein concentration was 5 μM. The analysis was carried out with a single-binding-site model. The experiments were repeated at least twice.

Acknowledgment. We thank Drs. Fabrice Fleury and Pierre Weigel for discussions and Dr. Kyoko Iwasaki-Yoshikane for CD measurements. This work was supported by grants from the Association pour la Recherche sur le Cancer [no. 3862], the Région de Pays de la Loire [MIAPS] and [CIMATH], the King Abdullah University of Science and Technology [KUK-11-008-23 to B.N.], and Swiss National Science Foundation [31003A-116275 to A.S.]. J.N. is a recipient of a Ph.D. fellowship from the Ligue Contre le Cancer Comité Loire Atlantique.

Supporting Information Available: Raw data on ITC calorimetry analysis of Rad51/BRC peptide interaction. MALDI-TOF mass spectrometry data and purity of peptides. RP-HPLC analytical data of noncommercial modified peptides. This material is available free of charge via the Internet at http://pubs.acs.org.

References

(1) Friedberg, E. C.; Walker, G. C.; Siede, W.; Wood, R. D.; Schultz, R. A.; Ellenberger, T. *DNA Repair and Mutagenesis*; ASM Press: Washington, DC, 2006.
(2) Haaf, T.; Golub, E. I.; Reddy, G.; Radding, C. M.; Ward, D. C. Nuclear foci of mammalian Rad51 recombination protein in somatic cells after DNA damage and its localization in synaptonemal complexes. *Proc. Natl. Acad. Sci. U.S.A.* **1995**, *92*, 2298–2302.
(3) Sonoda, E.; Sasaki, M. S.; Buerstedde, J. M.; Bezzubova, O.; Shinohara, A.; Ogawa, H.; Takata, M.; Yamaguchi-Iwai, Y.; Takeda, S. Rad51-deficient vertebrate cells accumulate chromosomal breaks prior to cell death. *EMBO J.* **1998**, *17*, 598–608.

(4) Vispe, S.; Cazaux, C.; Lesca, C.; Defais, M. Overexpression of Rad51 protein stimulates homologous recombination and increases resistance of mammalian cells to ionizing radiation. *Nucleic Acids Res*. **1998**, *26*, 2859–2864.
(5) Christodoulopoulos, G.; Malapetsa, A.; Schipper, H.; Golub, E.; Radding, C.; Panasci, L. C. Chlorambucil induction of HsRad51 in B-cell chronic lymphocytic leukemia. *Clin. Cancer Res*. **1999**, *5*, 2178–2184.
(6) Henning, W.; Sturzbecher, H. W. Homologous recombination and cell cycle checkpoints: Rad51 in tumour progression and therapy resistance. *Toxicology* **2003**, *193*, 91–109.
(7) Yanagisawa, T.; Urade, M.; Yamamoto, Y.; Furuyama, J. Increased expression of human DNA repair genes, XRCC1, XRCC3 and RAD51, in radioresistant human KB carcinoma cell line N10. *Oral Oncol*. **1998**, *34*, 524–528.
(8) Maacke, H.; Opitz, S.; Jost, K.; Hamdorf, W.; Henning, W.; Kruger, S.; Feller, A. C.; Lopens, A.; Diedrich, K.; Schwinger, E.; Sturzbecher, H. W. Overexpression of wild-type Rad51 correlates with histological grading of invasive ductal breast cancer. *Int. J. Cancer* **2000**, *88*, 907–913.
(9) Choudhury, A.; Zhao, H.; Jalali, F.; Al Rashid, S.; Ran, J.; Supiot, S.; Kiltie, A. E.; Bristow, R. G. Targeting homologous recombination using imatinib results in enhanced tumor cell chemosensitivity and radiosensitivity. *Mol. Cancer Ther*. **2009**, *8*, 203–213.
(10) Collis, S. J.; Tighe, A.; Scott, S. D.; Roberts, S. A.; Hendry, J. H.; Margison, G. P. Ribozyme minigene-mediated RAD51 down-regulation increases radiosensitivity of human prostate cancer cells. *Nucleic Acids Res*. **2001**, *29*, 1534–1538.
(11) Ito, M.; Yamamoto, S.; Nimura, K.; Hiraoka, K.; Tamai, K.; Kaneda, Y. Rad51 siRNA delivered by HVJ envelope vector enhances the anti-cancer effect of cisplatin. *J. Gene Med*. **2005**, *7*, 1044–1052.
(12) Ko, J. C.; Hong, J. H.; Wang, L. H.; Cheng, C. M.; Ciou, S. C.; Lin, S. T.; Jheng, M. Y.; Lin, Y. W. Role of repair protein Rad51 in regulating the response to gefitinib in human non-small cell lung cancer cells. *Mol. Cancer Ther*. **2008**, *7*, 3632–3641.
(13) Ohnishi, T.; Taki, T.; Hiraga, S.; Arita, N.; Morita, T. In vitro and in vivo potentiation of radiosensitivity of malignant gliomas by antisense inhibition of the RAD51 gene. *Biochem. Biophys. Res. Commun*. **1998**, *245*, 319–324.
(14) Bignell, G.; Micklem, G.; Stratton, M. R.; Ashworth, A.; Wooster, R. The BRC repeats are conserved in mammalian BRCA2 proteins. *Hum. Mol. Genet*. **1997**, *6*, 53–58.
(15) Bork, P.; Blomberg, N.; Nilges, M. Internal repeats in the BRCA2 protein sequence. *Nat. Genet*. **1996**, *13*, 22–23.
(16) Wong, A. K.; Pero, R.; Ormonde, P. A.; Tavtigian, S. V.; Bartel, P. L. RAD51 interacts with the evolutionarily conserved BRC motifs in the human breast cancer susceptibility gene BRCA2. *J. Biol. Chem*. **1997**, *272*, 31941–31944.
(17) Chen, C. F.; Chen, P. L.; Zhong, Q.; Sharp, Z. D.; Lee, W. H. Expression of BRC repeats in breast cancer cells disrupts the BRCA2−Rad51 complex and leads to radiation hypersensitivity and loss of G(2)/M checkpoint control. *J. Biol. Chem*. **1999**, *274*, 32931–3295.
(18) Davies, A. A.; Masson, J. Y.; McIlwraith, M. J.; Stasiak, A. Z.; Stasiak, A.; Venkitaraman, A. R.; West, S. C. Role of BRCA2 in control of the RAD51 recombination and DNA repair protein. *Mol. Cell* **2001**, *7*, 273–282.
(19) Galkin, V. E.; Esashi, F.; Yu, X.; Yang, S.; West, S. C.; Egelman, E. H. BRCA2 BRC motifs bind RAD51−DNA filaments. *Proc. Natl. Acad. Sci. U.S.A*. **2005**, *102*, 8537–8542.
(20) Nomme, J.; Takizawa, Y.; Martinez, S. F.; Renodon-Corniere, A.; Fleury, F.; Weigel, P.; Yamamoto, K.; Kurumizaka, H.; Takahashi, M. Inhibition of filament formation of human Rad51 protein by a small peptide derived from the BRC-motif of the BRCA2 protein. *Genes Cells* **2008**, *13*, 471–481.
(21) Pellegrini, L.; Yu, D. S.; Lo, T.; Anand, S.; Lee, M.; Blundell, T. L.; Venkitaraman, A. R. Insights into DNA recombination from the structure of a RAD51−BRCA2 complex. *Nature* **2002**, *420*, 287–293.
(22) Rajendra, E.; Venkitaraman, A. R. Two modules in the BRC repeats of BRCA2 mediate structural and functional interactions with the RAD51 recombinase. *Nucleic Acids Res*. **2010**, *38*, 82–96.
(23) Ababou, A.; Ladbury, J. E. Survey of the year 2004: literature on applications of isothermal titration calorimetry. *J. Mol. Recognit*. **2006**, *19*, 79–89.
(24) Jelesarov, I.; Bosshard, H. R. Isothermal titration calorimetry and differential scanning calorimetry as complementary tools to investigate the energetics of biomolecular recognition. *J. Mol. Recognit*. **1999**, *12*, 3–18.
(25) Benson, F. E.; Stasiak, A.; West, S. C. Purification and characterization of the human Rad51 protein, an analogue of *E. coli* RecA. *EMBO J*. **1994**, *13*, 5764–5771.
(26) Liu, Y.; Stasiak, A. Z.; Masson, J. Y.; McIlwraith, M. J.; Stasiak, A.; West, S. C. Conformational changes modulate the activity of human RAD51 protein. *J. Mol. Biol*. **2004**, *337*, 817–827.
(27) Bak-Jensen, K. S.; Andre, G.; Gottschalk, T. E.; Paes, G.; Tran, V.; Svensson, B. Tyrosine 105 and threonine 212 at outermost substrate binding subsites −6 and +4 control substrate specificity, oligosaccharide cleavage patterns, and multiple binding modes of barley alpha-amylase 1. *J. Biol. Chem*. **2004**, *279*, 10093–10102.
(28) Quemener, A.; Bernard, J.; Mortier, E.; Plet, A.; Jacques, Y.; Tran, V. Docking of human interleukin-15 to its specific receptor alpha chain: correlation between molecular modeling and mutagenesis experimental data. *Proteins* **2006**, *65*, 623–636.
(29) Tran, V.; Hoffmann, L.; Rabiller, C.; Tellier, C.; Dion, M. Rational design of a GH1 beta-glycosidase to prevent self-condensation during the transglycosylation reaction. *Protein Eng., Des. Sel*. **2010**, *23*, 43–49.
(30) Carreira, A.; Hilario, J.; Amitani, I.; Baskin, R. J.; Shivji, M. K.; Venkitaraman, A. R.; Kowalczykowski, S. C. The BRC repeats of BRCA2 modulate the DNA-binding selectivity of RAD51. *Cell* **2009**, *136*, 1032–1043.
(31) Shivji, M. K.; Mukund, S. R.; Rajendra, E.; Chen, S.; Short, J. M.; Savill, J.; Klenerman, D.; Venkitaraman, A. R. The BRC repeats of human BRCA2 differentially regulate RAD51 binding on single- versus double-stranded DNA to stimulate strand exchange. *Proc. Natl. Acad. Sci. U.S.A*. **2009**, *106*, 13254–13259.
(32) Sali, A.; Blundell, T. L. Comparative protein modelling by satisfaction of spatial restraints. *J. Mol. Biol*. **1993**, *234*, 779–815.
(33) Asensio, J. L.; Martin-Pastor, M.; Jimenez-Barbero, J. The use of CVFF and CFF91 force fields in conformational analysis of carbohydrate molecules. Comparison with AMBER molecular mechanics and dynamics calculations for methyl [alpha]-lactoside. *Int. J. Biol. Macromol*. **1995**, *17*, 137–148.
(34) Dinur, U., Hagler, A. T. In *Review of Computational Chemistry with Discover−InsightII Packages*; Lipkowitz, K. B., Boyd, D. B., Eds.; Accelrys: San Diego and New York, 1991.
(35) Kim, J. M.; Maraboeuf, F.; Kim, S. K.; Shinohara, A.; Takahashi, M. Effect of ions and nucleotides on the interactions of yeast Rad51 protein with single-stranded oligonucleotides. *J. Biochem*. **2001**, *129*, 469–475.
(36) Chabbert, M.; Lami, H.; Takahashi, M. Cofactor-induced orientation of the DNA bases in single-stranded DNA complexed with RecA protein. A fluorescence anisotropy and time-decay study. *J. Biol. Chem*. **1991**, *266*, 5395–5400.
(37) Di Capua, E.; Engel, A.; Stasiak, A.; Koller, T. Characterization of complexes between recA protein and duplex DNA by electron microscopy. *J. Mol. Biol*. **1982**, *157*, 87–103.